

**Estimation of the Electromagnetic Bias from  
Retracked TOPEX Data**

Ernesto Rodriguez and Jan M. Martin  
Jet Propulsion Laboratory  
California Institute of Technology.  
4800 Oak Grove Dr., Pasadena, CA 91109

## Abstract

We examine the EM bias by using retracked TOPEX altimeter data. In contrast to previous studies, we use a parametrization of the EM bias which does not make stringent assumptions about the form of the correction or its global behavior. We find that the most effective single parameter correction uses the altimeter estimated wind speed, but that other parametrizations, using a wave age related parameter of significant wave height may also significantly reduce the repeat pass variance. The different corrections are compared and their improvement of the TOPEX height variance is quantified.

## 1. Introduction

Ocean altimeters, such as the TOPEX altimeter, measure the power weighted mean surface height of the scatterers on the ocean surface. Experimentally, it has long been known that, because the wave troughs are brighter than the peaks for radar wavelengths, the mean electromagnetic surface measured by altimeters is lower than the true mean sea surface. This effect is known as the EM bias and was first reported by Yapple et al. [1971]. Subsequently, various investigators have tried to determine the behavior of the bias using both tower and airborne experiments [Walsh et al., 1989], [Walsh et al., 1991], [Hevizi et al., 1993], [Melville et al., 1991], and from satellite altimeter data itself [Born et al., 1982], [Douglas and Agreen, 1983], [Ray and Koblinsky, 1991], [Witter and Chelton, 1991], [Fu and Glazman, 1991]. The tower and airborne experimental results have never agreed exactly with the satellite derived results. This may be due to several factors, of which we mention three: 1) the tower and airborne data is not representative of the open ocean conditions; 2) the altimeter data was corrupted with other geophysical effects, such as ionosphere delays or orbit errors, which could be accidentally correlated to the bias itself due to the geographical distribution of the error; 3) the parametrization of the bias itself was not correct.

The parametrization of the bias has been a source of some controversy. The early results took a constant fraction of the significant wave height,  $H_{1/3}$ . Later theoretical and experimental developments have indicated that other parameters should be included. The first theoretical explanation of the bias by Jackson [1979] suggested a connection to the sea

surface skewness. This theoretical explanation used geometrical optics scattering, as did the later investigation of Glazman and Srokosz [1991], which suggested that the EM bias was a function of the wave age for wind driven seas. Rodriguez et al. [1992] showed that one could not neglect diffraction effects in the calculation of the bias, and that the modulation of small waves by larger waves also played an important part in the determination of the bias and its frequency dependence. In that paper, we also noted theoretical behavior at high wind speed  $U$  which has been observed in experimental data [Walsh et al., 1991]. Based on empirical analysis of the Geosat data, Witter and Chelton [1991] have suggested that the bias may, in fact, depend on  $H_{1/3}$  nonlinearly. It seems to be a fair assessment of the situation to say that the optimal parametrization is not yet resolved.

The TOPEX data provide an excellent source for estimating the EM bias since long wavelength errors, which could contaminate the bias estimate, have been reduced (see this issue) so that the EM bias signature is now clearer. In this paper, we estimate the magnitude and functional dependence of the EM bias using a new technique which does not make strong assumptions about the functional dependence of the bias. Furthermore, we use retracked altimeter data [Rodriguez and Martin, this issue], which further eliminates contamination due to processing biases. We examine several EM bias parametrization and assess their efficacy by their ability to reduce the repeat pass variance. Both of the TOPEX frequencies, Ku and C band, are included in the analysis.

## 2. EM Bias Estimation Procedure

On dimensional grounds, the EM bias must be of the form

$$h_{EM} = \sum \alpha_i(\eta) L_i \quad (1)$$

where  $\eta$  represents (possibly multiple) dimensionless parameters characteristic of the ocean conditions, and  $L_i$  are length scales intrinsic to the ocean surface wave spectrum or the boundary layer. Wind driven ocean spectra are characterized [Phillips, 1980] by an outer length scale, typically proportional to  $U^2/g$ , an inner scale, given by the characteristics of the small wave dissipation mechanism, and, possibly, an intermediate scale [Glazman and

Weichman, 1989] [Phillips, 1985] characteristic of wave breaking. The outer scale determines the significant wave height ( $H_{1/3}$ ), which can be used to characterize it. The wave breaking scale is probably a function of the wind speed ( $U$ ) and  $H_{1/3}$ . The inner length scale is not very well understood, but there are indications [Jaehne and Riemer, 1990] that it may be a weak function of both  $U$  and  $H_{1/3}$ . For situations where swell dominates, the suitable length scales are the swell amplitude, which determines  $H_{1/3}$ , and its wavelength. The altimeter has access to only one length scale of the surface,  $H_{1/3}$ , which is characteristic of the outer spectral scales and, therefore, we use it, as our characteristic length scale.

While there are various possible parameters characteristic of sea surface conditions (such as temperature), there are only two non-dimensional quantities which can be constructed from the altimeter measurements. The first quantity, the effective surface slope variance, can be obtained through measurements of  $\sigma_0$ , the normalized radar cross section, which, for nadir incidence, is a strong function of the slope variance. Rather than use this quantity directly, we use the altimeter determined wind speed,  $U$ , which it determines uniquely. This is in accord with the classical results of Cox and Munk [1954] who showed a near-linear relationship between the surface slope variance and the wind speed. It also agrees with the parametrization used to determine the empirical behavior of the EM bias by Walsh and coworkers [Walsh et al., 1991] and by Melville and coworkers [Melville et al., 1991]. To determine the wind speed from the  $\sigma_0$  measurements, we used the wind speed model function derived by Witter and Chelton [1991] for the Geosat altimeter and the  $\sigma_0$  measurements in the TOPEX Geophysical Data Record (GDR). There are some questions about the relative calibration between TOPEX and Geosat (P. Callahan, private communication), so that the wind speed shown here may not be the same as would be derived from Geosat data. This will not be of great importance, since the wind speed is merely used as a data derived parameter, which is a nonlinear function of  $\sigma_0$ . As long as the relationship is one-to-one, no information will be lost and the correction based on the GDR  $\sigma_0$  may be applied, and, for the convenience of the GDR user, we have parametrized our results with the GDR  $\sigma_0$  and the published Witter-Chelton [1991] wind speed model.

The other non-dimensional quantity which can be derived from the altimeter measurements, the “pseudo-wave age”, is proportional to the ratio of the wind kinetic energy to the wave potential energy:

$$\rho \equiv \frac{U}{\sqrt{gH_{1/3}}} \quad (2)$$

This quantity has been used to characterize the wave age for developing waves [Janssen et al., 1976][Glazman and Pilorz, 1990], and is thus a determinant of the outer scale of the wave spectrum. Fu and Glazman [1991] have shown that the Geosat altimeter repeat pass height variance could be reduced by including a function of  $\rho$ .

Finally, Witter and Chelton [1991] have presented evidence that the functional dependence of  $\alpha$  for Geosat might be also a function of  $H_{1/3}$  itself. While hard to justify on dimensional grounds, this correction proved empirically successful and we also examine it here.

Of course, due to wind-wave coupling, these three parameters are far from being independent, especially for wind driven seas. Figure 1 presents the empirical correlation coefficient between these parameters as a function of latitude for the data set used in this study. This figure shows that the wind speed and  $\rho$  are always highly correlated, while the wind speed and  $H_{1/3}$  are more correlated at higher latitudes, where most of the wave generation is local, than at the equatorial zone, where outside swell can dominate the locally generated waves.

We model the observed altimeter height as

$$h^{(i)} = h_T + \alpha(\eta^{(i)})H_{1/3}^{(i)} + n^{(i)} \quad (3)$$

for the  $i$ th pass, where  $h_T$  is the true sea surface height and  $n$  represents measurement noise, Taking the differences with the sea surface heights measured by the next pass over the same region, and assuming that the sea surface height has not changed, the repeat pass difference will be given by

$$h^{(i+1)} - h^{(i)} = \alpha(\eta^{(i+1)})H_{1/3}^{(i+1)} - \alpha(\eta^{(i)})H_{1/3}^{(i)} + (n^{(i+1)} - n^{(i)}) \quad (4)$$

Notice that this assumption is better for TOPEX, whose repeat pass period is ten days, than for Geosat, which had a seventeen day repeat pass period.

To make further progress, we parametrize the function  $\alpha$  as follows

$$\alpha(\eta) = \sum_{i=0}^N \alpha_n f_n(\eta) \quad (5)$$

where the  $\alpha_n$  are unknown constants obtained by minimizing the repeat pass variance. The basis functions,  $f_n$ , have traditionally been taken to be low order polynomials in  $\eta$ : Born et al. [1982] and Douglas and A green [1983] choose  $f_n$  to be a constant, while Walsh et al. [1991] and Melville et al. [1991] have taken it to be a second order polynomial in  $U$ . We believe this assumption may overly constrain the functional form of  $\alpha$  and prefer to use local (in  $\eta$ ) basis functions, rather than the nonlocal polynomials. We have chosen the linear interpolation basis functions defined by

$$f_n(\eta) = 1 - \frac{|\eta - \eta_n|}{\Delta\eta} \quad (6)$$

when the result is positive, and zero otherwise. The basis functions were separated by uniform intervals in  $\eta$ :

$$\eta_n = n\Delta\eta + \eta_0 \quad 0 \leq n \leq N \quad (7)$$

Table 1 presents the values used for  $\Delta\eta$ ,  $\eta_0$ , and  $N$  for the various geophysical parameters used,

The use of localized basis functions allows for an arbitrary functional dependence in  $\alpha$  as long as the separation between basis functions is such that  $\Delta\alpha/\alpha \ll \Delta\eta/\eta$ . The disadvantage of localized basis functions is that many more fitting parameters need to be estimated than for global basis functions. However, we have used twenty-three cycles of TOPEX data for our fitting, so that the formal errors in the parameters are quite small compared to the desired accuracy.

An alternate method for determining the functional dependence of the EM bias on a surface parameter was proposed by Witter and Chelton [1991]. In their method, a mean ocean surface is constructed using the available data. The sea surface height differences of

each repeat pass with respect to this mean surface are then binned against the value of the parameter for the given pass, and the results are fit as a linear function of the difference between  $H_{1/3}$  for that pass minus the mean value of  $H_{1/3}$ . In this procedure, a separate  $\alpha$  is derived for each parameter bin. From equation ( 3 ), the height difference will be given by

$$h^{(i)} - \langle h \rangle = \alpha(\eta_{(i)})H_{1/3}^{(i)} - \langle \alpha(\eta)H_{1/3} \rangle \quad (8)$$

where  $\langle \rangle$  indicates averaging over all the passes. It is not clear that, in general, this expression is a global function of  $\eta_i$  only. In particular, correlations between  $\eta$  and  $H_{1/3}$ , or geographical dependence of the mean values can introduce unwanted artifacts. Nevertheless, as was shown by Witter and Chelton [1991], it is possible to use this technique to detect nonlinear trends in the behavior of  $\alpha$  with  $\eta$ , although the universality of the derived functional form is not guaranteed.

We used the retracked sea surface heights described by Rodriguez and Martin (this issue) to avoid introducing the unwanted systematic effects found in the TOPEX Geophysical Data Record (GDR). To reduce the effects of surface dynamics, we used only repeat pass differences between cycles neighboring in time. The data set consisted of retracked heights for cycles 3-27 (excluding cycles 20 and 16), including the GDR tropospheric and tidal corrections.

As was first reported by P. Gaspar in the TOPEX verification meeting (persona] communication), the estimated FM bias depends strongly on what fraction of the inverse barometer correction is applied. The inverse barometer correction accounts for the static depression of sea level due to atmospheric pressure loading. Since the ocean response is dynamic, it is not clear exactly how this correction should be applied. Wahr et al. [1993] found that the Geosat sea surface height variance was minimized when only 60% of the static correction was applied. In this study, we varied the percent of the correction applied and, as we report below, found that for TOPEX the variance is minimized when the full static correction is applied. This agrees with independent results obtained by L. Fu and coworkers (private communication) using minimization of cross-over differences.

The ionospheric correction potential has a large impact on the estimated EM bias. As we show below, this is not important at Ku-band. However, we found that for the C-band altimeter, not applying the correction results in unphysical estimates for the magnitude and sign of the EM bias due to the accidental correlation between the ionospheric electron content and the geographical distribution of significant wave height. The results presented here were obtained after applying the ionospheric correction. This is not without its dangers since the ionospheric correction is obtained from the difference between the Ku- and C-band ranges, and is thus potentially incestuous. However, as shown by D. Imel (this issue), there is good agreement between the TOPEX ionospheric measurements and the independent DORIS measurements. In addition, the corrections are derived from the altimeter height estimates, while we use the retracked height estimates. Nevertheless, to test the validity of this approach, we compared the estimated EM bias when the ionosphere was weak (height correction less than 4 cm), using or withholding the ionospheric correction, and found good agreement with our estimates using the full data set. As a further precaution, we neglected any set of passes whose variance was greater than  $400 \text{ cm}^2$  when averaged over the entire data set.

To estimate the fitting coefficients, we used the sequential Householder accumulation method described by Lawson and Hanson [1974]. We estimated the number of independent samples by empirically deriving the sea surface height correlation function and estimating the correlation distance. As a compromise between different geographical regions, we assumed that an independent sample was obtained every 36 sec (or approximately 200 km) and subsampled the data accordingly.

### 3. Results and Discussion

We estimated both the EM bias correction and the residual bias left in the data after applying the Ku- and C-band EM bias corrections used in the GDR. The functional fits for the GDR sea surface heights, which are basically the sea surface heights for the Ku-band altimeter, are presented in Figure 2 for the three fitting parameters discussed above. Figure 2a shows that the wind speed dependence of the fitting function follows the

GDR Ku-band model function quite closely in the wind speed region for all wind speeds, but there are some significant deviations for small and large values of wind speed. These same deviations appear in the fit to the residual, providing an independent confirmation of the fitting result.

The results of following the Witter-Chelton procedure for estimating the bias are also shown in Figure 2. While the agreement for the estimated bias is poor, especially for regions where low wind speeds dominate, the agreement for the estimated residual correction is good. This seems to indicate that the assumptions implicit in the Witter-Chelton method may introduce systematic differences when the wind speed is small compared to the average ocean wind speed ( $\sim 7\text{ m/s}$ ).

Figures 2b and 2c show the estimated behavior of the EM bias as a function of pseudo-wave age and significant wave height. The pseudo-wave age behavior mimics approximate y the wind speed behavior, which is what one would expect if there were no additional  $H_{1/3}$  dependence of the EM bias and significant wave height and wind speed were uncorrelated: i.e., if the ocean were swell dominated. The behavior of the bias with  $H_{1/3}$  seems to be quite unphysical and we argue below that this may be due to instrument error.

Table 2 presents the reduction in repeat pass variance after applying various corrections. The correction implemented on the GDR indeed reduces the variance and the variance reduction is maximized when the full barometer correction is applied. From figure 2a, we expect that given the mean ocean wind speed ( $\sim 7\text{ m/s}$ ) and  $H_{1/3}$  ( $\sim 2\text{ m}$ ) the order of magnitude reduction should be cm the order of  $\sim (5\text{ cm})^2$ , rather than the observed value  $\sim (3.5\text{ cm})^2$ . The wind speed correction seems to give marginally better variance reduction than any of the other single parameter corrections ( $\sim (5.6\text{ cm})^2$ ), while all of the parameters give approximately equivalent variance reduction when applied as residual corrections to the GDR EM bias correction.

Figure 3 shows the effect of the ionospheric correction and the inverse barometer correction on the estimated Ku-band EM bias. As expected, the ionospheric correction has a small effect. On the other hand, the inverse barometer effect has a substantial impact on

the estimated bias. This is probably due to the correlation between surface pressure and wind speed or significant wave height.

To further characterize the bias, we subdivided the data into three latitude bands corresponding roughly to the southern ( $-66^\circ$  to  $-20^\circ$ ), equatorial ( $-20^\circ$  to  $20^\circ$ ), and northern ( $20^\circ$  to  $66^\circ$ ) oceans. Figure 4 presents the results for the fitting function and Table 3 for the variance reduction. The wind speed dependence of the bias and its residuals exhibits a uniform behavior throughout the globe, with the exception of the high wind speed behavior in the equatorial band. However, the number of data points in this range is so small that the results are probably not statistically significant.

The pseudo-wave age dependence of the EM bias, on the other hand, exhibits significantly different behavior in the equatorial region. The dependence on  $\rho$  has the same form as in the higher latitudes, but the correction is about 1/2% greater in the equatorial region. This is probably due to the fact that this parameter is relevant for wind driven seas and the significant wave height in the equatorial region may have a strong swell component which was generated outside the region.

The significant wave height behavior of the estimated bias and the residual bias behaves in a fashion which is not consistent for any of the latitude bands. Furthermore, the formal estimation errors are much greater than for the other two parameters, and the variance reduction is smaller, indicating that there is a great deal of scatter in the trend. These observations suggest that we are observing an effect which is not driven by ocean physics but, rather, by some possible instrumental effect. The magnitude of the effect cannot be accounted for by the differences found between the GDR and retracked heights [Rodriguez and Martin, this issue]. In fact, the significant wave height dependence estimated using the GDR height exhibits trends which are quite similar to the ones reported here. We have not yet found an explanation for this behavior.

We have also examined EM bias functional forms which depend on two parameters. Since the significant wave height and wind speed are correlated, it is not possible to obtain

reliable estimates for a full two-dimensional fitting function. We have adopted the *ansatz*

$$h_{EM} = [\alpha(\eta) + \beta(\zeta)]H_{1/3} \quad (9)$$

where  $\alpha$  and  $\beta$  are different functional forms and  $\eta$  and  $\zeta$  are different parameters. Table 2 shows that applying this correction reduces the repeat pass variance by a small amount which may not be statistically significant. The shape of the estimated curves does not change much when the parameters are  $U$  and  $H_{1/3}$ . However, when the parameters are  $U$  and  $\rho$ , one notices that, away from the equatorial region, the low and high wind speed behavior seems to agree more closely with the experimentally observed behavior, while the  $\rho$  contribution is greatest for small (large wave age or swell domination) and large (small wave age) values of  $\rho$ , while for the most commonly occurring values of wave development. In the equatorial region, however, a significantly different trend is observed, again probably indicating the different relationship between wind and waves in this region.

Figure 6 and Table 4 present the EM bias estimation results for the C-band altimeter. This behavior is qualitatively similar to the one for Ku-band. However, there is a slower tapering of the bias with increasing  $U$  and  $\rho$ . This agrees qualitatively with experimental results [Walsh et al., 1991]. However, the overall level of the bias seems to be lower than the ones observed. Due to the uncertainties introduced by the application of the ionospheric correction, we cannot assess how significant this is. However, Table 2 shows that applying the correction estimated here significantly reduces the C-band repeat pass variance.

#### 4. Conclusions

We have examined the EM bias for the TOPEX altimeter as a function of various parametrization and frequencies. The bias correction applied to the GDR data provides an effective correction in the sense that the repeat pass variance is reduced. However, slightly different corrections, based on a variety of geophysical parameters provide even greater variance reduction. Perhaps the simplest correction, and the single parameter correction which most reduces the repeat pass variance, is a correction based on the estimated wind speed alone. We give the numerical values for the fitting parameters for this parametrization

in Table 5. However, other corrections based on pseudo-wave age and  $H_{1/3}$  also seem to provide similar amounts of variance reduction. The correction based on  $H_{1/3}$  does not seem physical in that it varies significantly between hemispheres. It may be related to an instrument effect, but we have not been able to account for it. The pseudo-wave age correction shows uniform behavior away from the equatorial region, but its behavior changes in this region. We argue that this may be due to the presence of swell. Including two parameters into the fit does not significantly reduce the repeat pass variance.

### Acknowledgement

The research described in this paper was carried out by the Jet Propulsion Laboratory, California Institute of Technology, under contract with the National Aeronautics and Space Administration. We would like to thank D. Chelton, L.L. Fu, P. Gaspar, R. Glazman, R. Stewart, and E. Walsh for their helpful comments during the TOPEX verification workshop and subsequently. We would also like to thank K. Wiedman for her useful comments.

### References

- Born, G.H., Richards, M. A., Rosborough, "An empirical determination of the effects of sea state bias on SEA SAT altimetry," J. Geophys. Res., 87, C5, 3221-3226, 1982,
- Cox, C., and Munk, W., "Statistics of the sea surface derived from sun glitter," J. Mar. Res., 13, 198-227, 1954.
- Douglas, B. C., and Agreen, R. W., "The sea state correction for GEOS3 and SEASAT satellite altimeter data," J. Geophys. Res., 88, C3, 1983.
- Fu, L.L., and Glazman, R., "The effect of the degree of wave development on the sea state bias in radar
- Glazman, R.E., Pilorsz, S.H., "Effects of sea maturity on satellite altimeter measurements," J. Geophys. Res., 95, NC3, 2857-2870, 1990.

- Glazman, R.E., and Srokosz, M.A., "Equilibrium wave spectrum and sea state bias in satellite altimetry," *J. Phys. ocean.*, 21, 11, 1609-1621, 1991.
- Glazman, R.E., and Weichman, P.B., "Statistical geometry of a small surface patch in a developed sea", *J. Geophys. Res.*, 94, C4, 4998-5010, 1989.
- Hasselmann, K., Ross, D.B., Muller, P., Sell, W., "A parametric wave prediction model," *J. Phys. Ocean.*, 6, 200-228, 1976.
- Hevizi, L.G., Walsh, E.J., McIntosh, R.E., Vandemark, D., Hines, D. E., "Electromagnetic bias in sea-surface range measurements at frequencies of the TOPEX Poseidon satellite", *IEEE Geosci.*, 31(2), 376-388, 1993.
- Jackson, F. C., "The reflection of impulses from a nonlinear random sea," *J. Geophys. Res.*, 84, C8, 4934-4939, 1979.
- Jaehne, H., and Riemer, K. S., "Two-dimensional wave number spectra of small scale water surface waves," *J. geophys. res.*, 95, C7, 11,531-11,546, 1990.
- Lawson, C.J., and Hanson, **R. J., Solving Least Squares Problems**, Prentice Hall, New Jersey, 1976.
- Melville, W. K., Stewart, R. H., Keller, W. C., Kong, J. A., Arnold, D. V., "Measurements of electromagnetic bias "in radar altimetry," *J. Geophys. Res.*, 96, NC3, 4915-4924, 1991.
- Phillips, O.M., **The Dynamics of the Upper Ocean**, Cambridge university Press, New York, 1980.
- Phillips, O. M., "Spectral and statistical properties of the equilibrium range in wind-generated gravity waves," *J. Fluid Mech.*, 156, 505-531, 1985.
- Ray, R.D., and Koblinsky, C. J., "On the sea-state bias of the Geosat altimeter," *J. Atmos. Oc.*, 8, 3, 397-408, 1991.

- namec E., Kim, Y., and Martin, J. M., "The effect of small-wave modulation on the electromagnetic bias," *J. Geophys. Res.*, 97, 2, 2379-2389, 1992.
- VanDam, T. M., and Wahr, J., "The atmospheric load response of the ocean determined using Geosat altimeter data," *Geophys. J.*, 113, 1, 1-16, 1993.
- Walsh, E. J., Jackson, F. C., Hines, D. E., Piazza, C., Hevizi, L. G., "Frequency dependence of electromagnetic bias in radar altimeter sea-surface range measurements," *J. Geophys. Res.*, 96, NC11, 571-583, 1991.
- Walsh, E. J., Jackson, F. C., Uliana, E. A., Swift, R. N., "Observations of the electromagnetic bias in radar altimeter sea surface measurements," *J. Geophys. Res.*, 94, C10, 14,575-14,584, 1989.
- Witter, D. L., and Chelton, D. B., "A Geosat altimeter wind-speed algorithm and a method for altimeter wind-speed algorithm development," *J. Geophys. Res.*, 96, NC5, 8853-8860, 1991.
- Witter, D. L., and Chelton, D. B., "An apparent wave height dependence in the sea-state bias in Geosat altimeter range measurements," *J. Geophys. Res.*, 95, NC5, 8861-8867, 1991,
- Yaplee, B. S., Shapiro, A., Hammond, D. J., Au, B. D., Uliana, E. A., "Nanosecond radar observations of the ocean surface from a stable platform," *IEEE Trans. Geosci. Electron.*, GE-9, 171-174, 1971.

### Figure Captions

**Figure 1:** Correlation coefficient between the wind speed and  $\rho$  (diamonds) or  $H_{1/3}$  (pluses), as a function of latitude. Note the latitudinal dependence of the correlation with  $H_{1/3}$ , indicating the presence of non-locally generated waves in the tropics.

**Figure 2:** Estimated EM bias parametrized as a function of wind speed (a),  $\rho$  (b), and  $H_{1/3}$  (c). The dashed lines are the fitting functions for the estimated EM bias correction (crosses) and the residual correction to the GDR data (diamonds). The estimates for the same quantities using the method of Witter and Chelton are given by the triangles and squares, respectively. (a) also shows the GDR EM bias correction, Notice that it does not have the quadratic form described in the GDR handbook. This is due to the relative miscalibration of TOP X and Geosat, and its impact on the Witter-Chelton wind speed mode] function.

Figure 3: The effects of not applying the ionospheric correction (diamonds), or applying 60% of the tropospheric correction (squares) on the estimated wind speed dependence of the EM bias.

**Figure 4:** Latitude dependence of the EM bias estimates parametrized as a function of  $U$  (a),  $\rho$  (b), and  $H_{1/3}$ . The upper pannel shows the effect on the EM bias correction, while the lower pannel shows the effect on the residual correction.

Figure 5: Estimates of the simultaneous  $U$  (upper pannel) and  $\rho$  (lower pannel) dependence of the EM bias. The latitude bands are  $-66^\circ$ -  $-20^\circ$  (crosses),  $-20^\circ$ -  $20^\circ$  (triangles), and  $20^\circ$ - $66^\circ$  (diamonds).

Figure 6: As in Figure 2, but for the C-band altimeter.

Parameter	$N$	$\eta_0$	$\Delta\eta$
$U$	17	1 m/s	1 m/s
$P$	16	0.15	0.15
$H_{1/3}$	19	0.5 m	0.5 m

Table 1: Number of basis functions ( $=N+1$ ), minimum value of the fitting for the lowest basis function ( $\eta_0$ ), and separation between the centers of each basis function ( $\Delta\eta$ ), for the three fitting parameters: wind speed ( $U$ ), pseudo-wave age ( $\rho$ ), and significant wave height ( $H_{1/3}$ ).

Correction	% of Inverse Barometer	Variance Reduction (cm <sup>2</sup> )
TOPEX GDR	100	12.1
TOPEX GDR	60	4.1
TOPEX GDR	0	-80.2
u	100	31.4
u	60	24.9
TOPEX GDR & U	100	31.5
$\frac{U}{\sqrt{gH_{1/3}}}$	100	30.2
TOPEX GDR & $\frac{U}{\sqrt{gH_{1/3}}}$	100	31.6
$H_{1/3}$	100	30.4
TOPEX GDR & $H_{1/3}$	100	31.3
U & $\frac{U}{\sqrt{gH_{1/3}}}$	100	31.9
TOPEX GDR & U & $\frac{U}{\sqrt{gH_{1/3}}}$	100	31.9
U & $H_{1/3}$	100	32.0
TOPEX GDR & U & $H_{1/3}$	100	31.9

Table 2: TOPEX SS11 variance reduction for various EM bias corrections. The raw variance, without any EM bias corrections, is 134.8cm<sup>2</sup>. The percent of the inverse barometer effect correction applied is also varied. The TOPEX GDR ionospheric correction has been applied throughout.

Correction	Variance Reduction $\text{cm}^2$		
	-66°- -20° Lat.	-20°- 20° Lat.	20°-66° Lat.
$U$	34.9	19.2	37.7
$P$	33.1	19.3	39.8
$H_{1/3}$	33.4	18.7	37.3
$U$ & $\frac{U}{\sqrt{gH_{1/3}}}$	35.4	20.0	38.8

Table 3: Variance reduction for various corrections segregated by latitude bands, The repeat variances without any EM bias correction are given by 152.4 $\text{cm}^2$ , 90.4 $\text{cm}^2$ , and 148.0 $\text{cm}^2$ , in the same order as the one used in the table above.

Correction	Variance Reduction ( $\text{cm}^2$ )
TOPEX GDR	15.9
$u$	38.8
TOPEX GDR & $U$	39.1
$\frac{U}{\sqrt{gH_{1/3}}}$	38.4
TOPEX GDR & $\frac{U}{\sqrt{gH_{1/3}}}$	39.2
$H_{1/3}$	37.5
TOPEX GDR & $H_{1/3}$	39.1

Table 4: TOPEX C-band SSH variance reduction for various EM bias corrections. The raw variance, without any EM bias corrections, is 147.4 $\text{cm}^2$ . The full inverse barometer correction and the TOPEX GDR ionospheric corrections have been applied throughout. Any repeat pass whose variance, averaged over all the cycles of data used, is greater than 400  $\text{cm}^2$  has been rejected.

$U_n$	$\alpha_n$	$\sigma\alpha_n$
1.0	-1.599	$2.4 \times 10^{-3}$
2.0	-1.218	$2.0 \times 10^{-3}$
3.0	-1.424	$1.7 \times 10^{-3}$
4.0	-1.734	$1.5 \times 10^{-3}$
5.0	-1.996	$1.3 \times 10^{-3}$
6.0	-2.344	$1.2 \times 10^{-3}$
7.0	-2.490	$1.2 \times 10^{-3}$
8.0	-2.540	$1.2 \times 10^{-3}$
9.0	-2.645	$1.2 \times 10^{-3}$
10.0	-2.644	$1.2 \times 10^{-3}$
11.0	-2.549	$1.2 \times 10^{-3}$
12.0	-2.366	$1.2 \times 10^{-3}$
13.0	-2.216	$1.3 \times 10^{-3}$
14.0	-2.028	$1.3 \times 10^{-3}$
15.0	-1.689	$1.3 \times 10^{-3}$
16.0	-1.593	$1.7 \times 10^{-3}$
17.0	-1.516	$1.9 \times 10^{-3}$
18.0	-1.485	$2.4 \times 10^{-3}$

Table 5: Fitting coefficients for the wind speed basis expansion. The last parameter is the  $1\sigma$  formal estimate of the error of the fitting parameter  $\alpha_n$ ,  $U_n$  are the centers for the linear interpolation basis functions

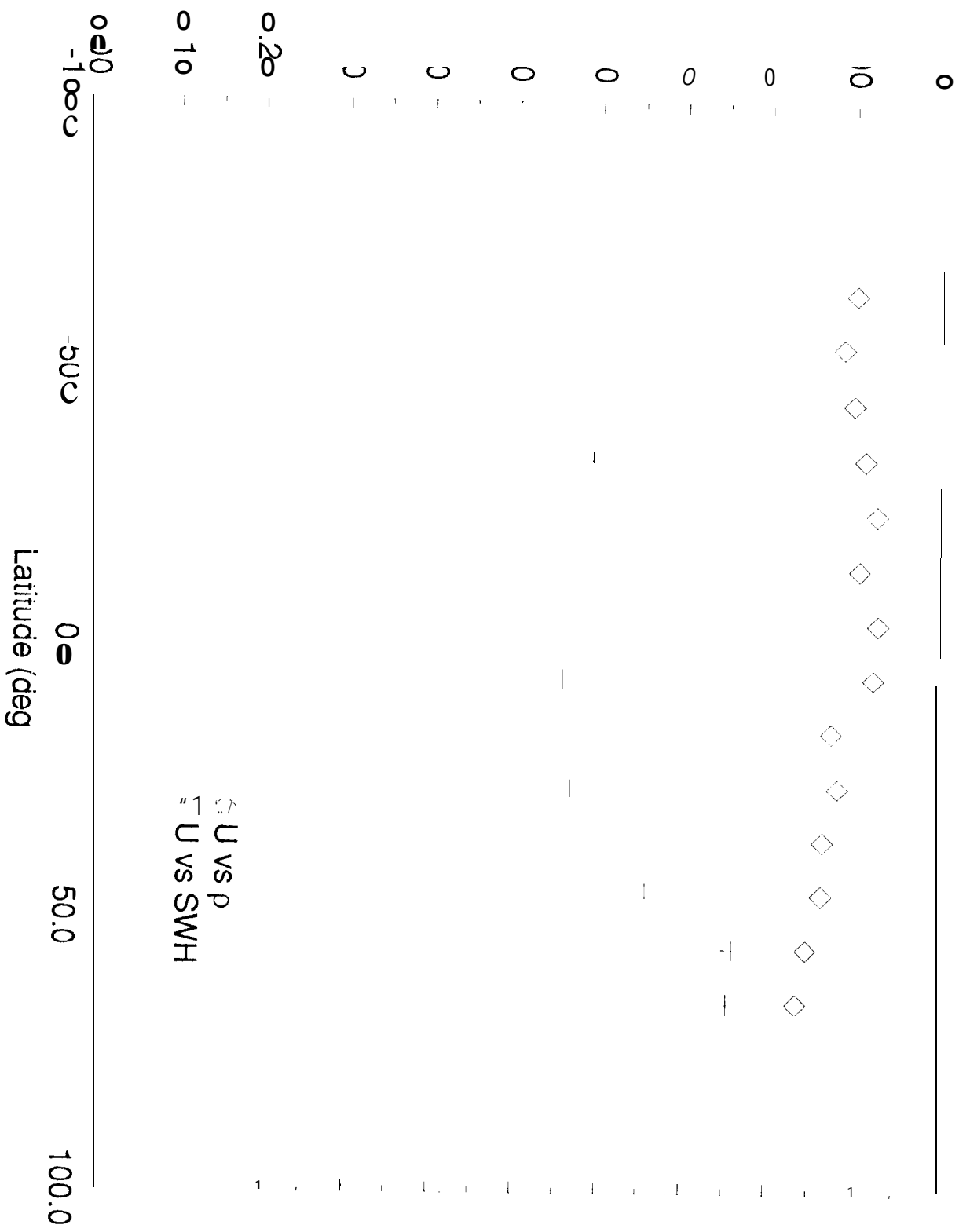


Figure 1

# Wind Speed Dependence of EM Bias

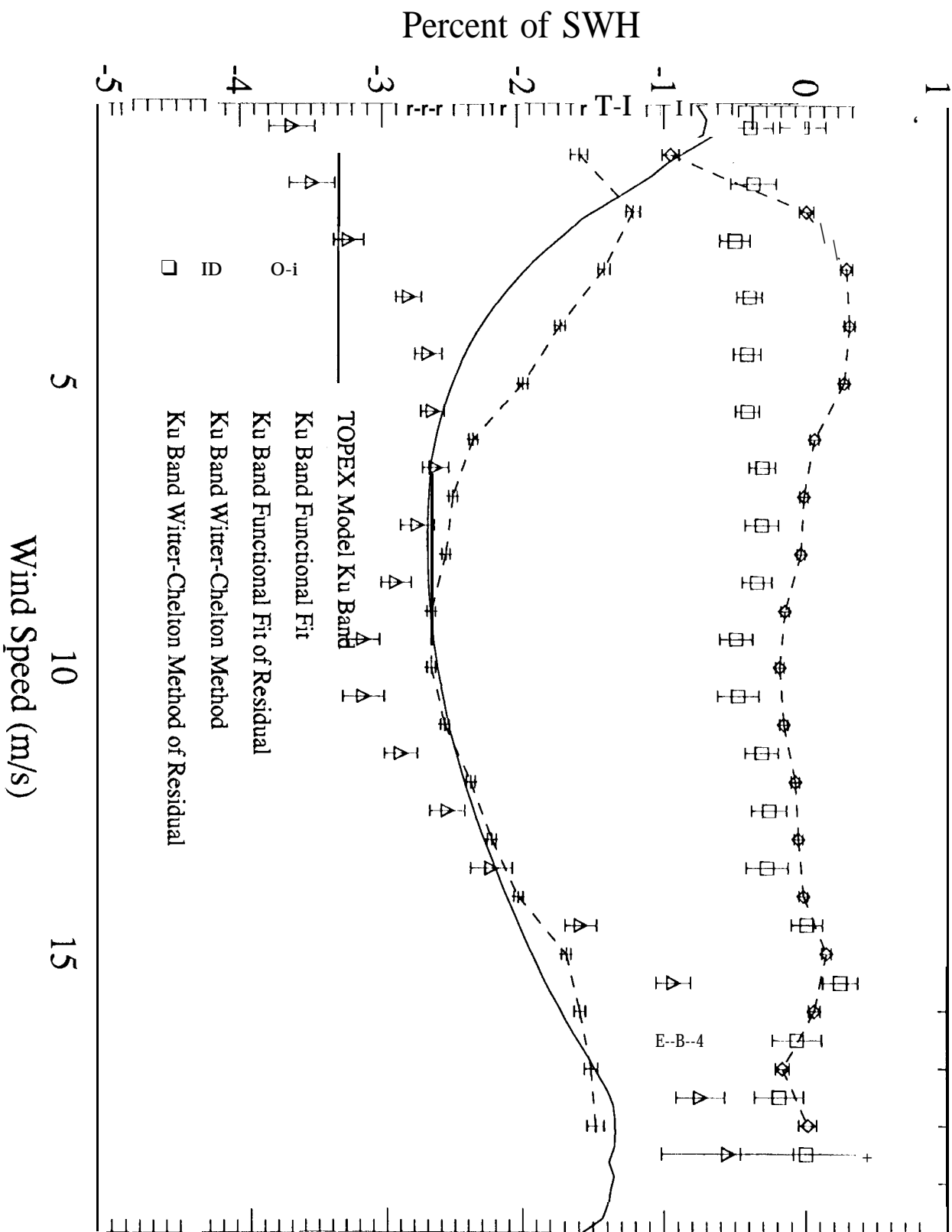


Figure 2a

# Pseudo-Wave Age Dependence of EM Bias

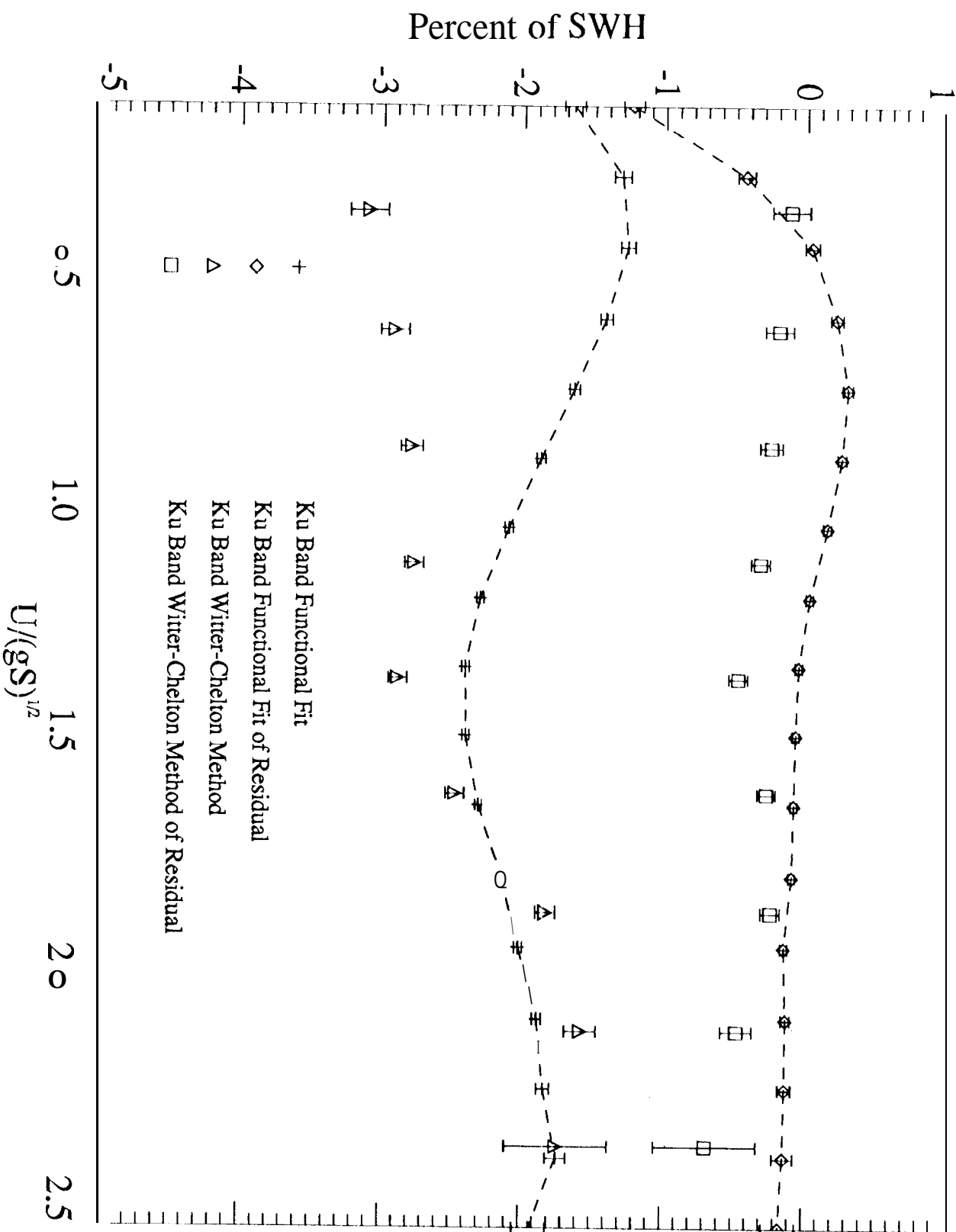


Figure 2a

# SWH Dependence of EM $\epsilon$ ias

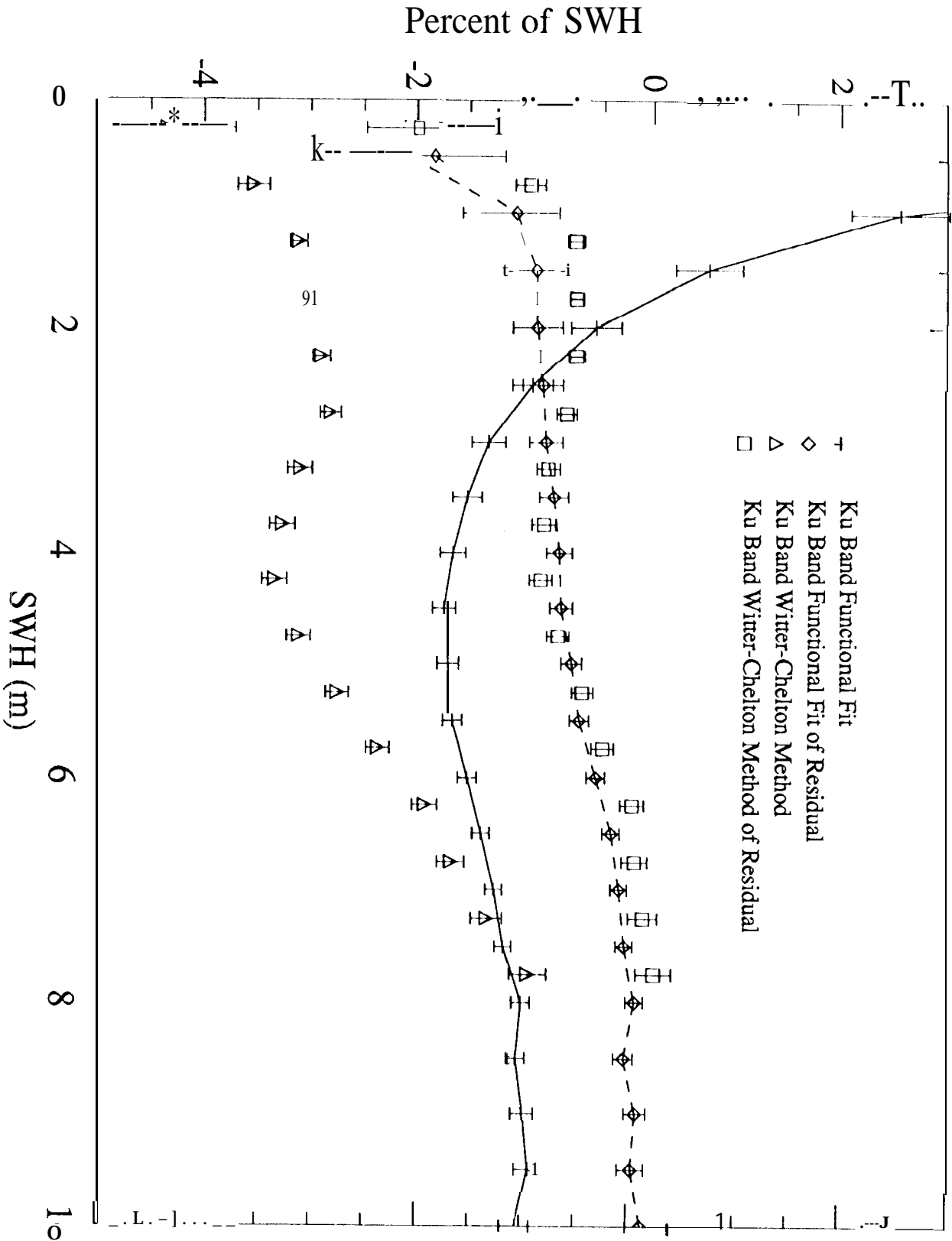


Figure 2c

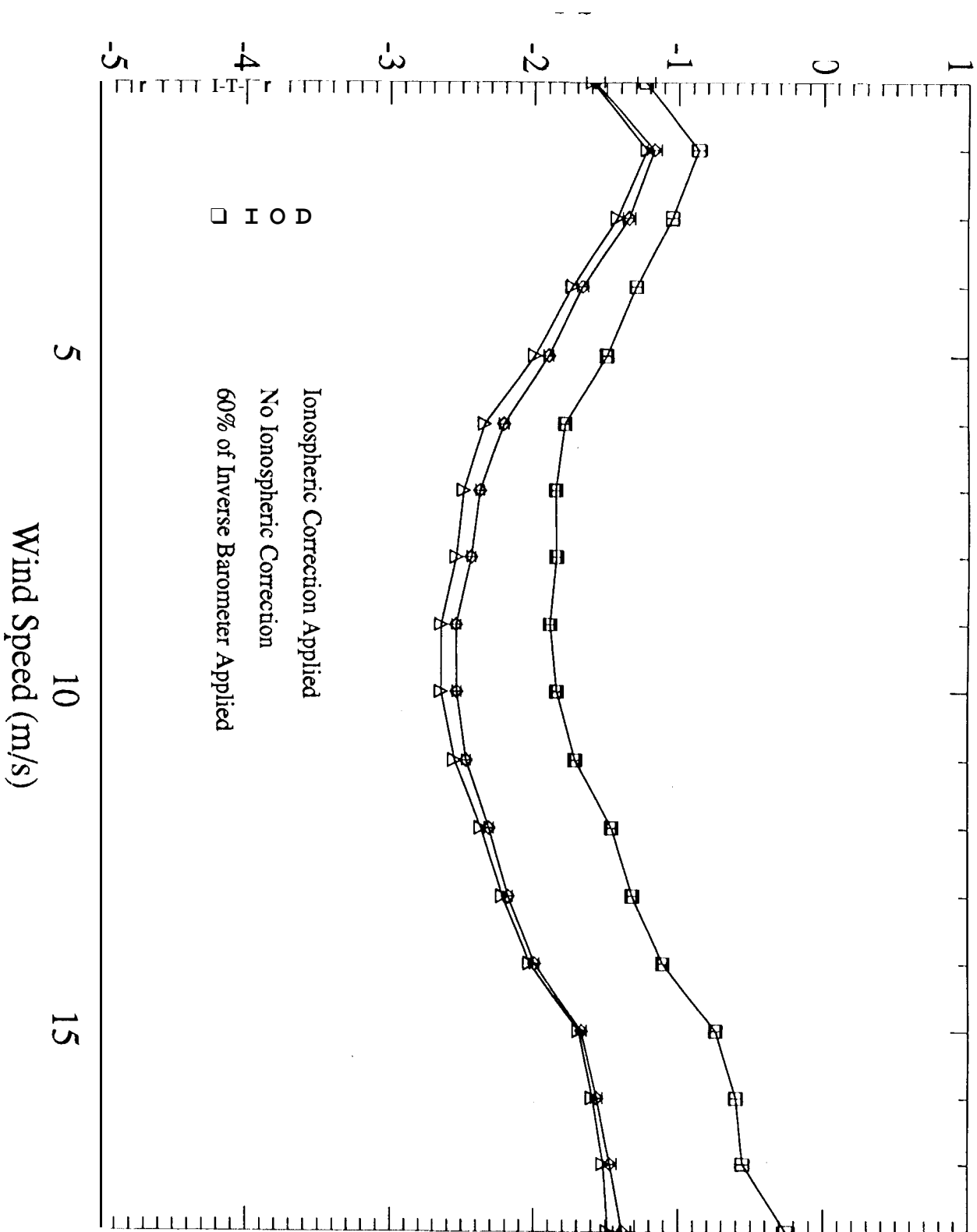
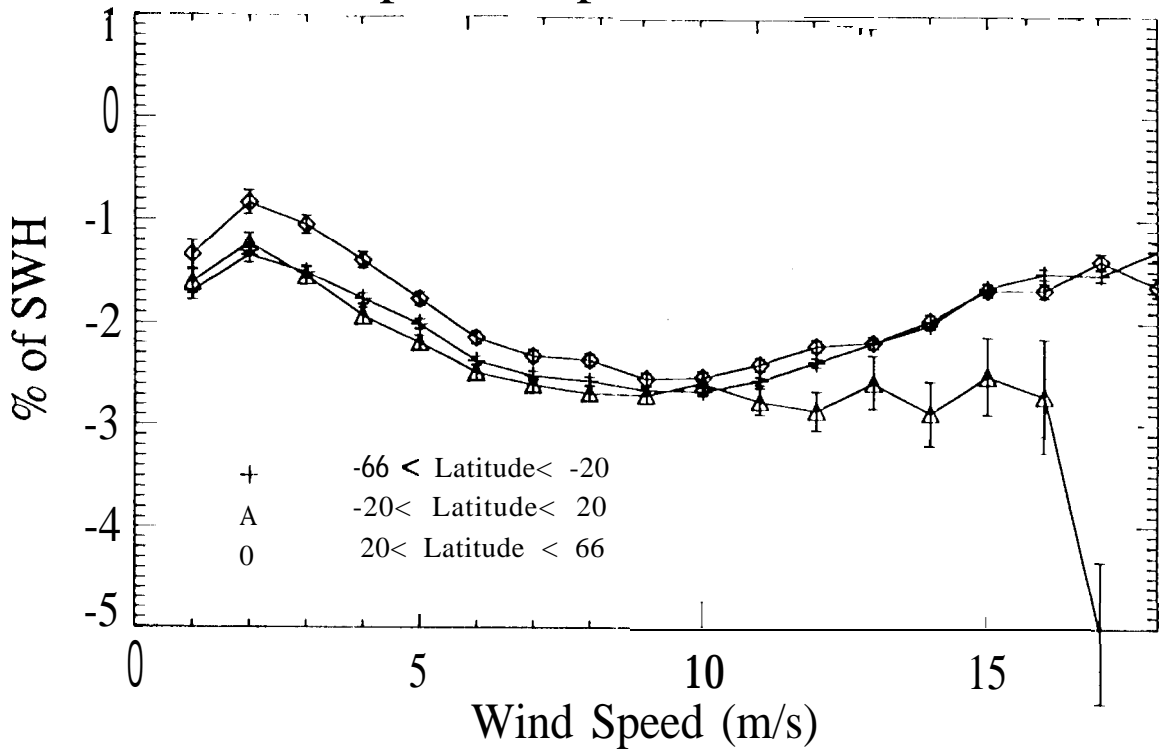


FIG. 3

# Wind Speed Dependence of EM Bias



# Wind Speed Dependence of EM Bias Residuals

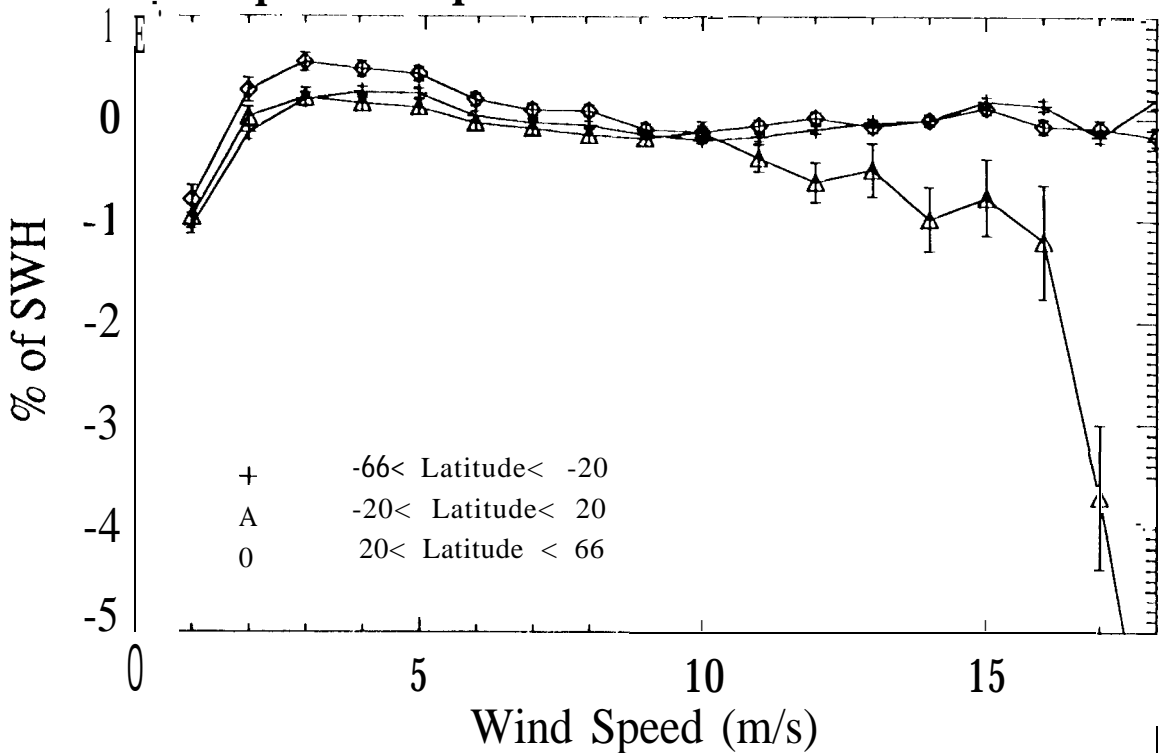
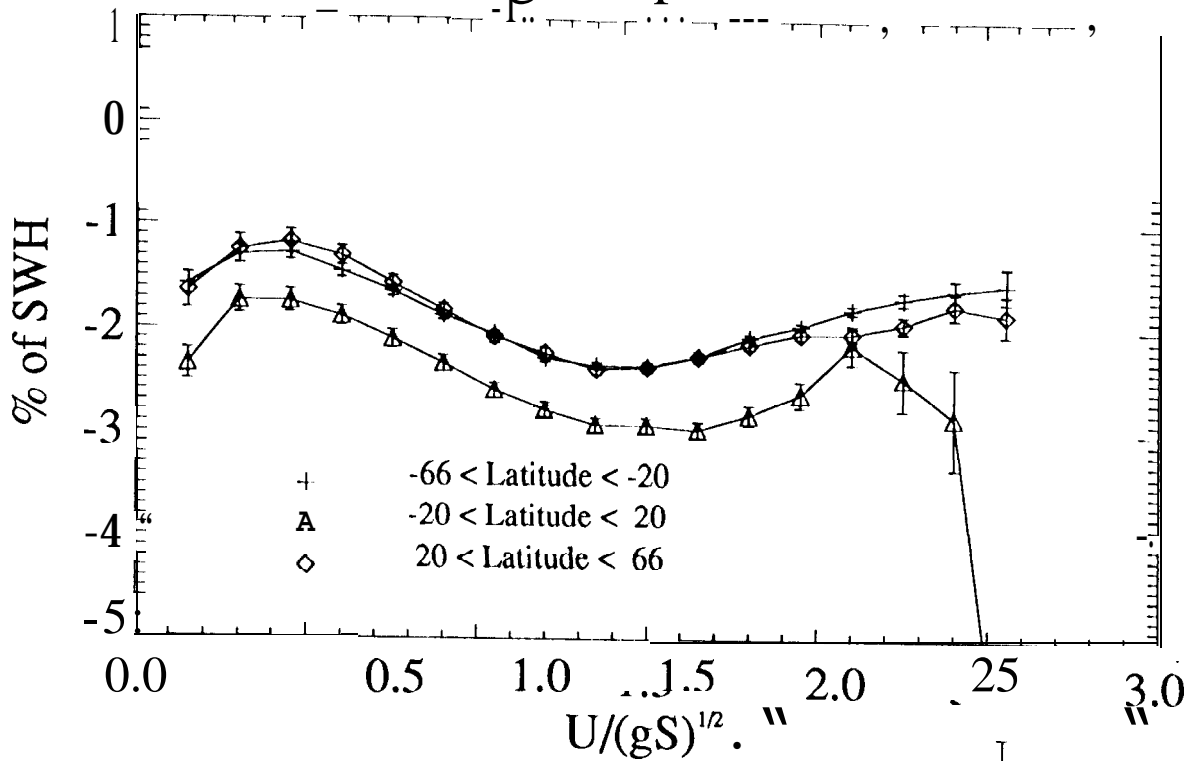


Figure 4a

### Pseudo-Wave Age Dependence of EM Bias



### Pseudo-Wave Age Dependence of EM Bias

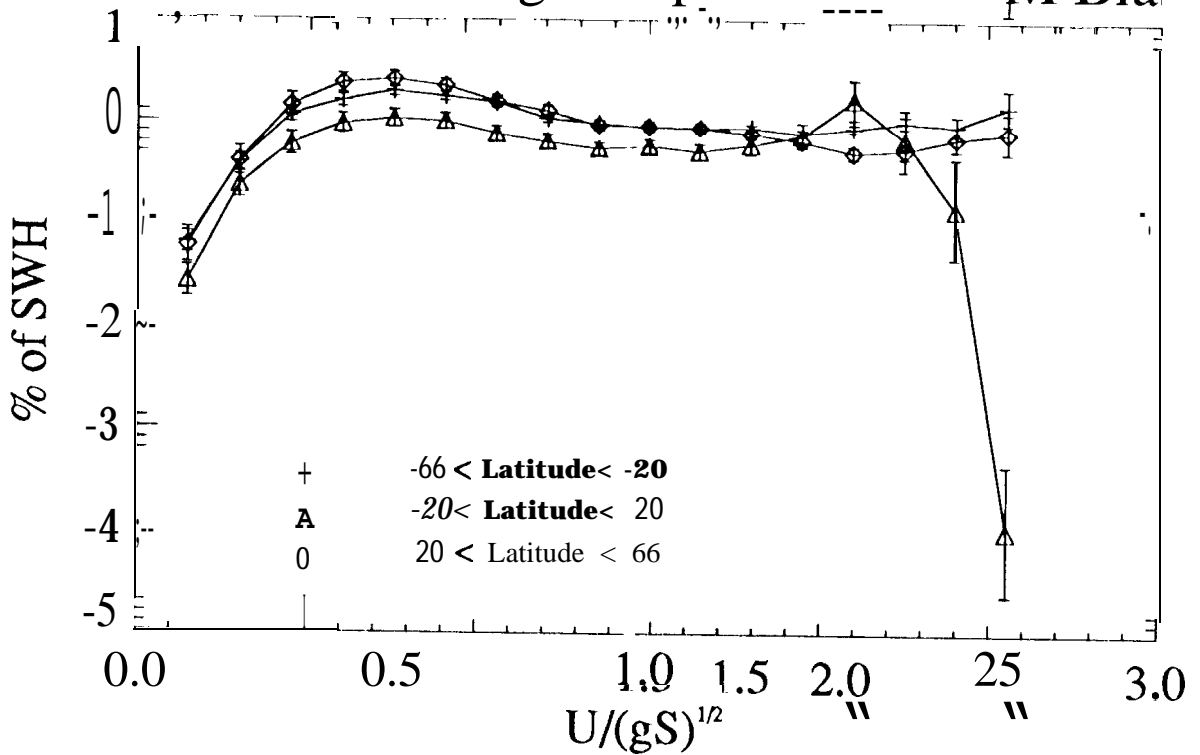


Figure 4b

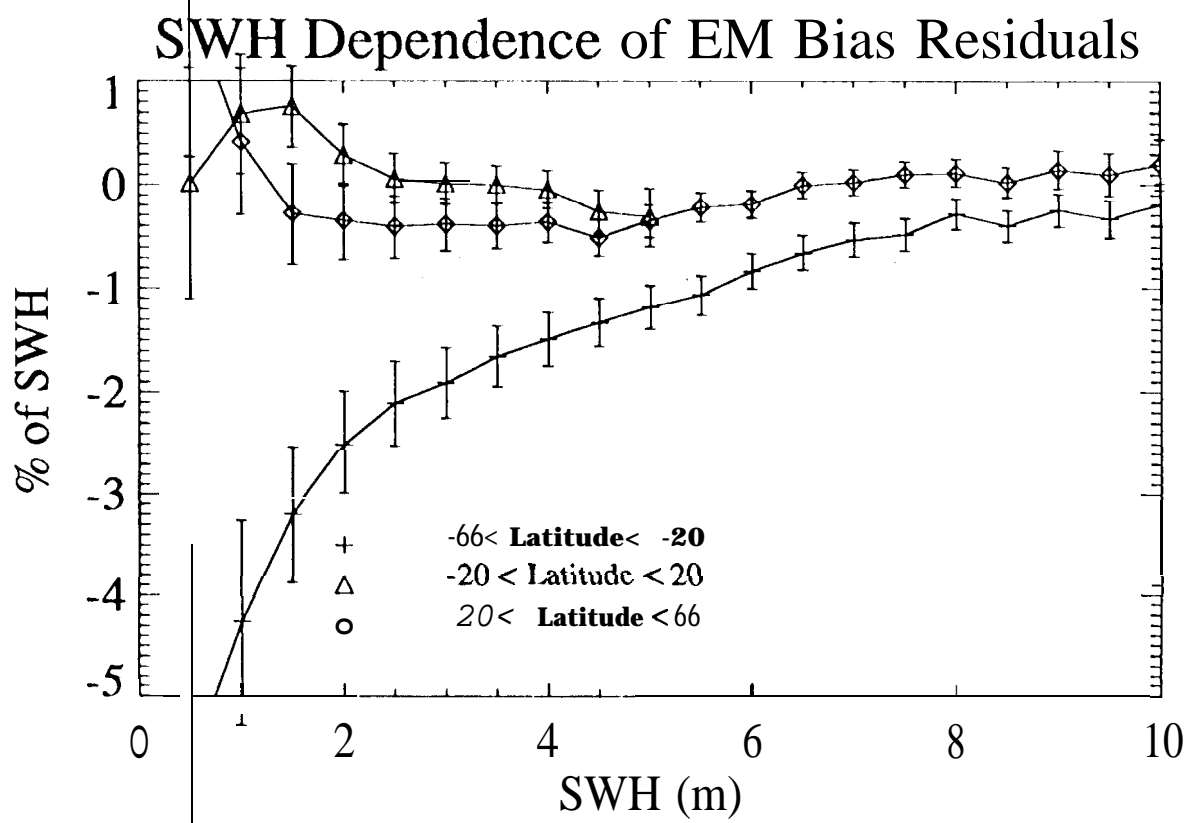
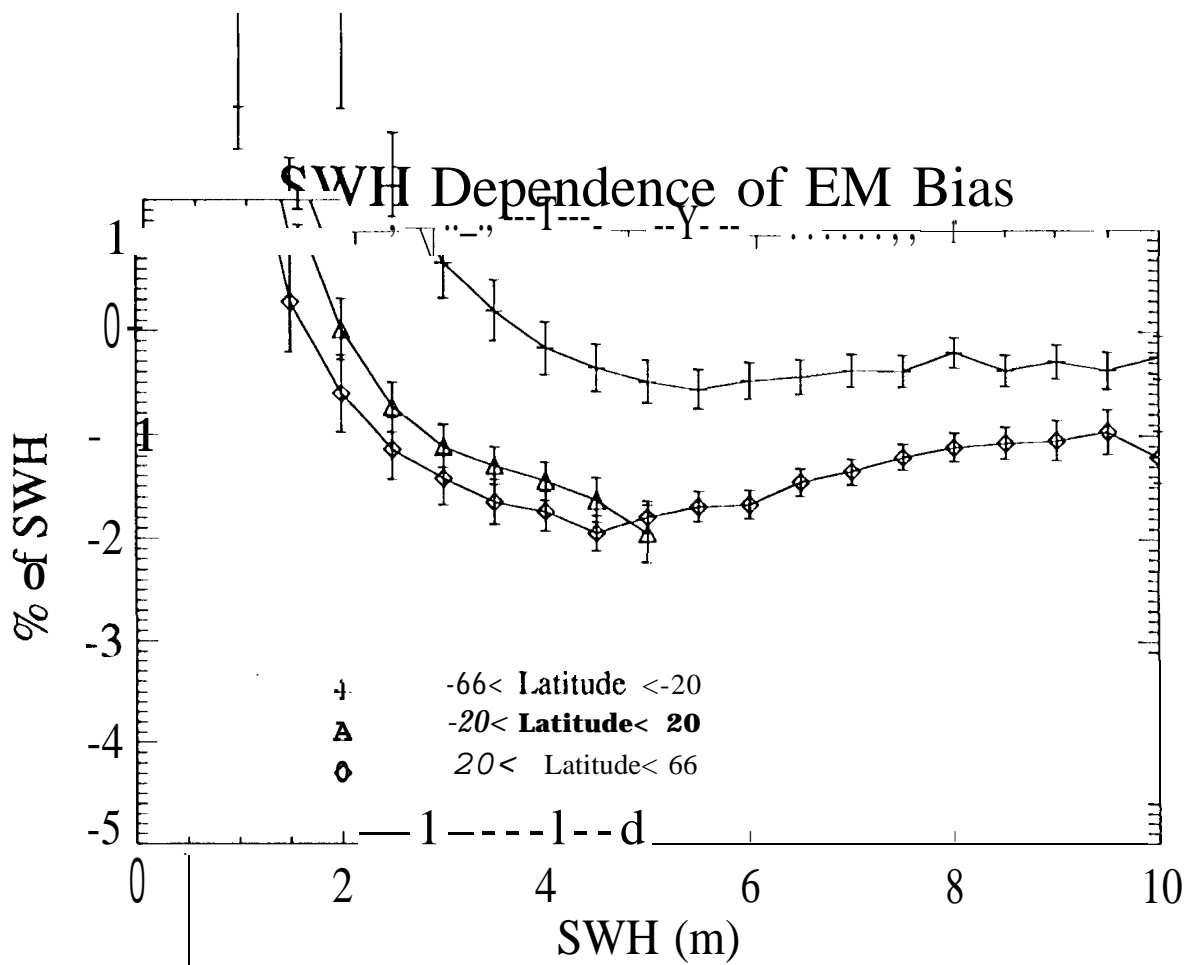


Figure Ac

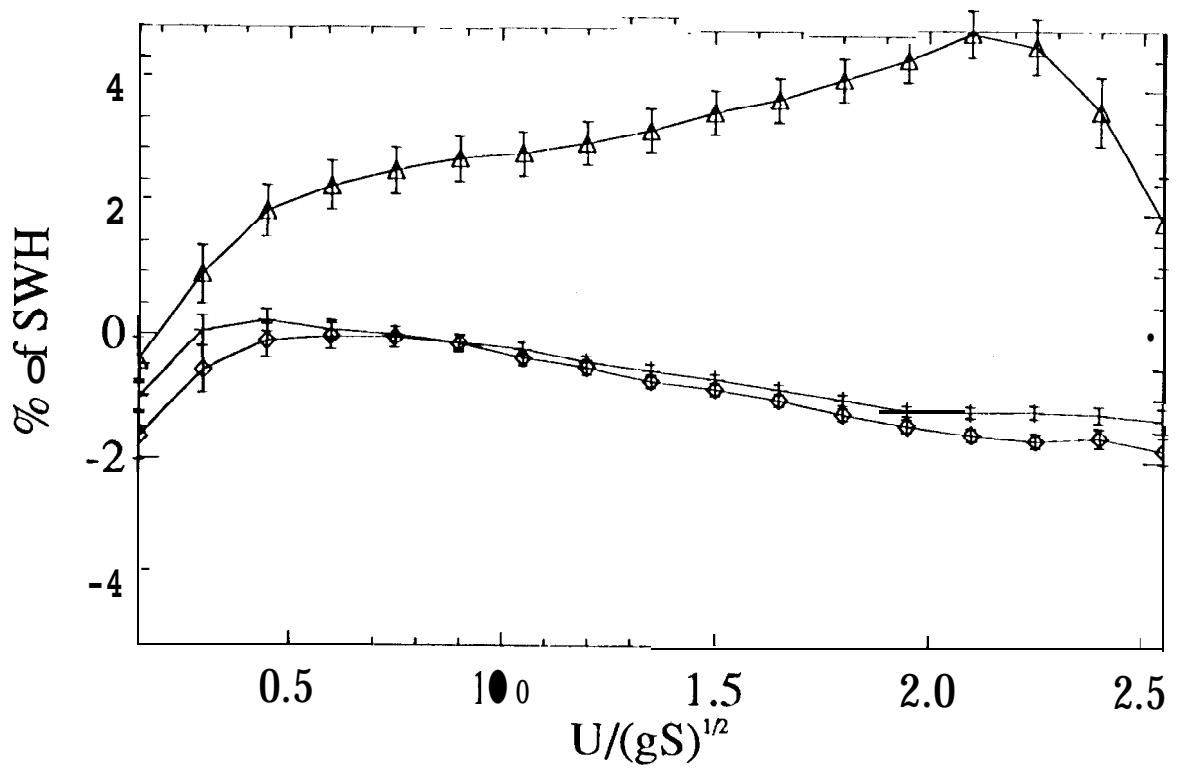
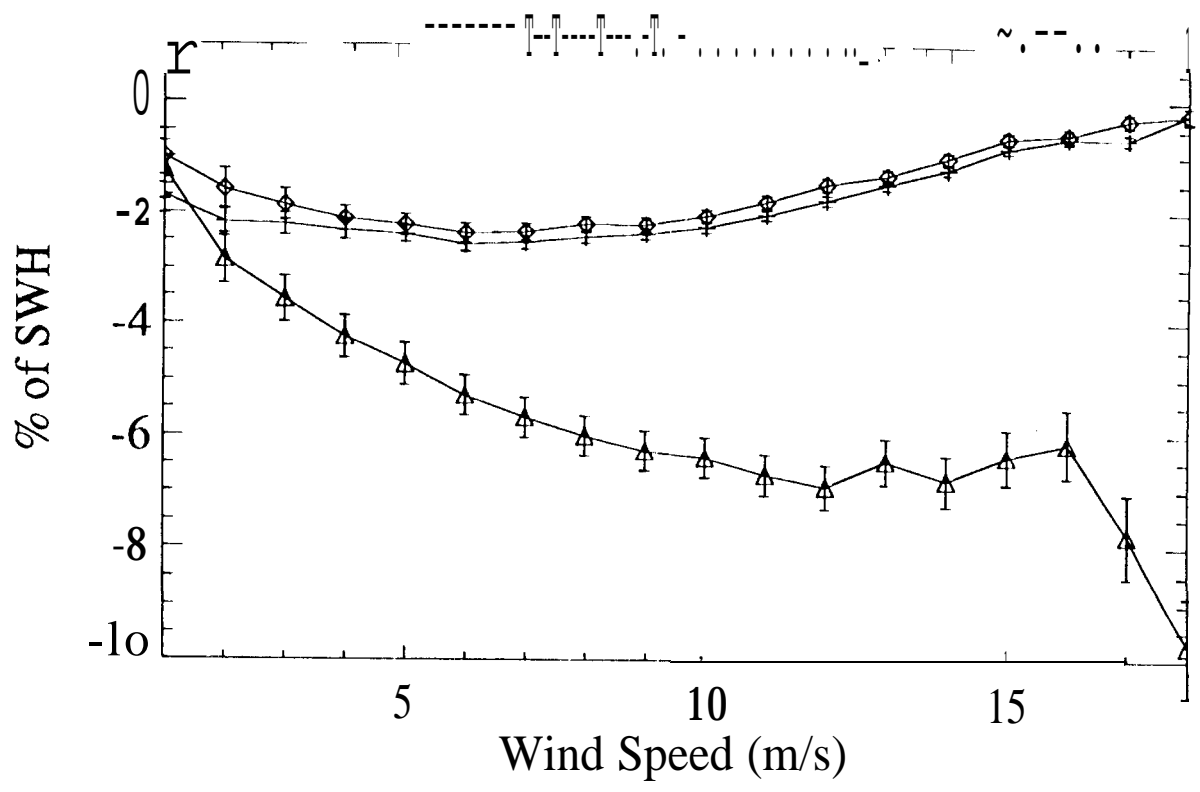


Figure 5

# Wind Speed Dependence of EM Bias

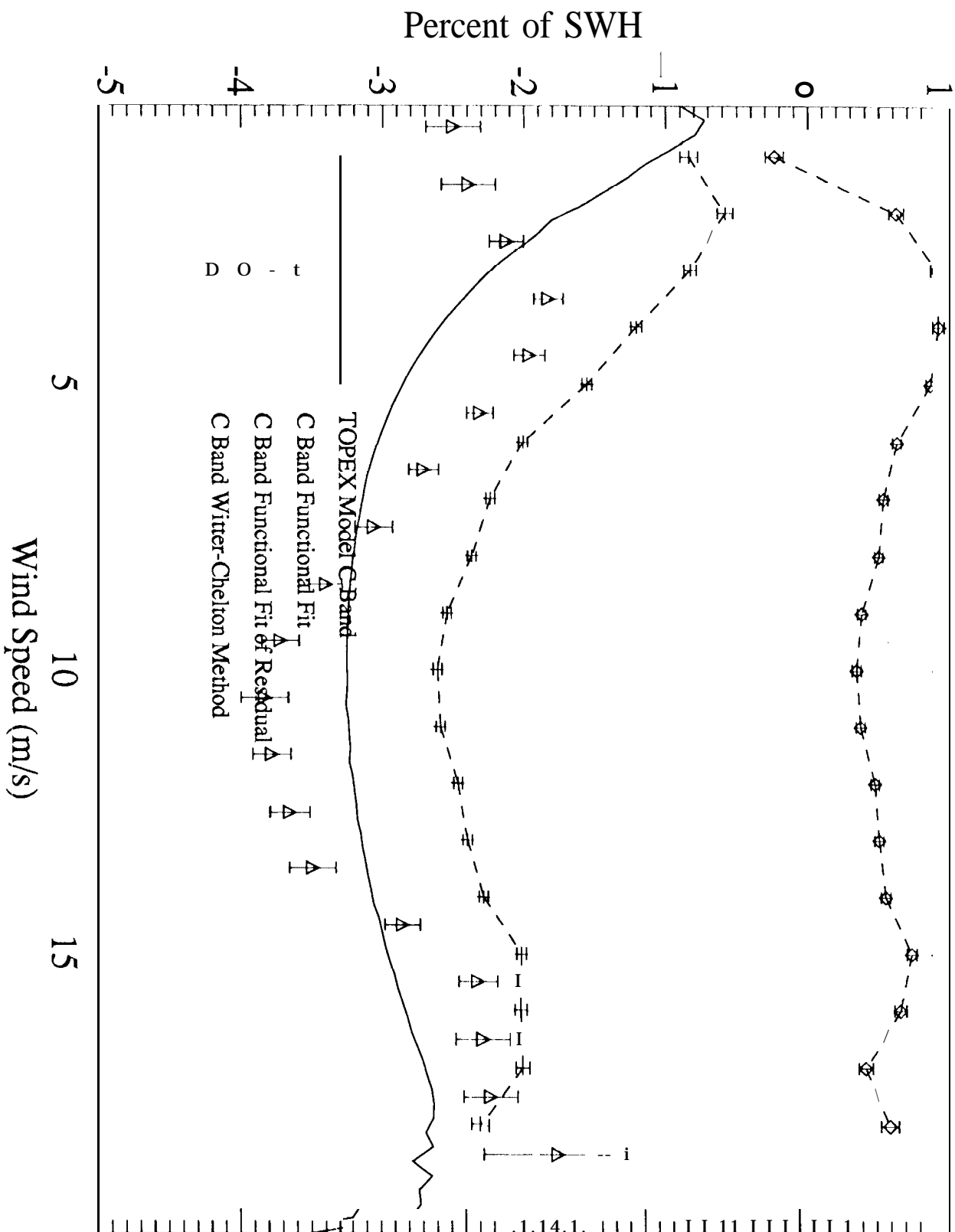


Figure 5a

# SWH Dependence of EM $\beta$ ias

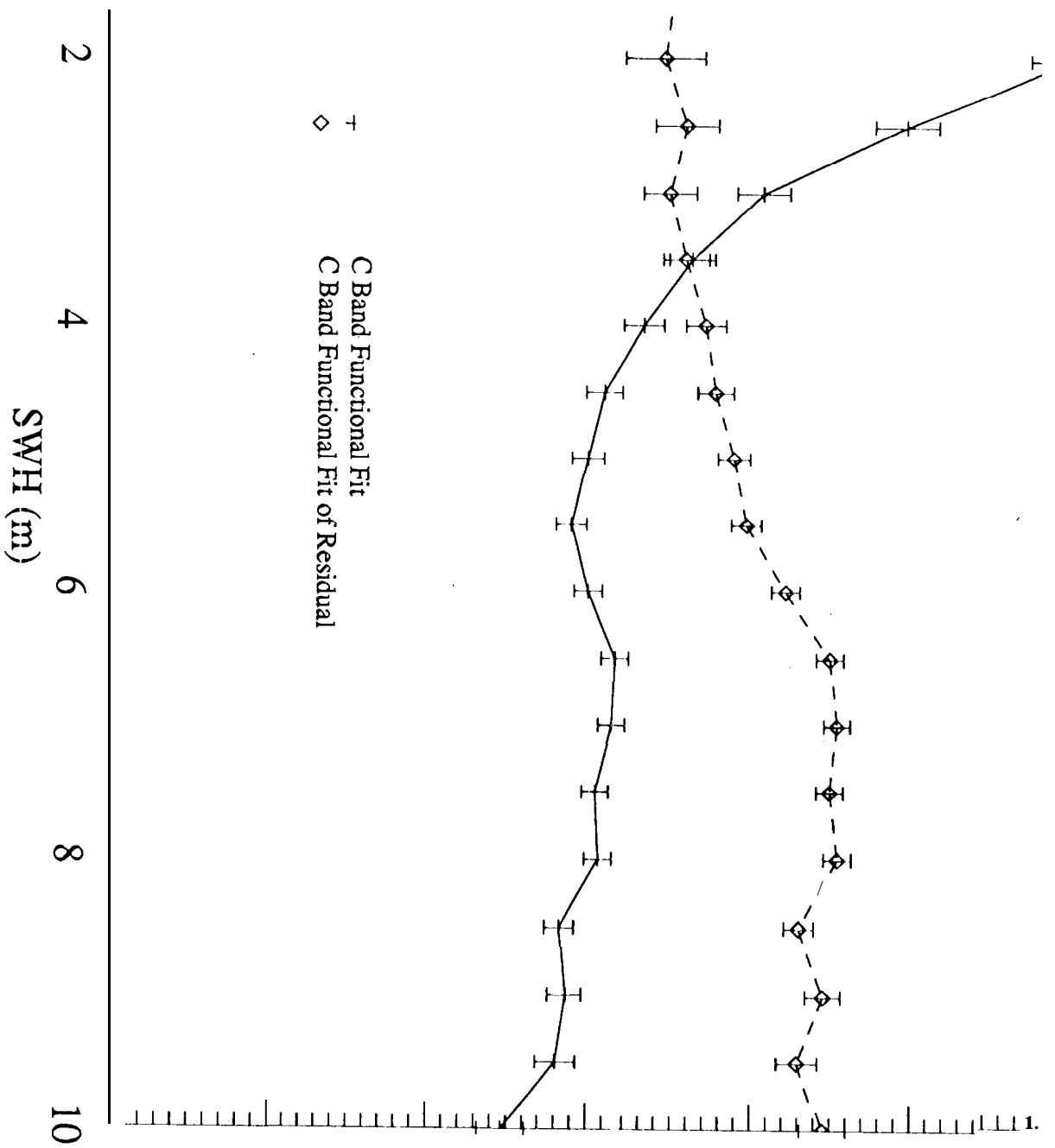


Figure 6c

# Pseudo-Wave Age Dependence of EM Bias

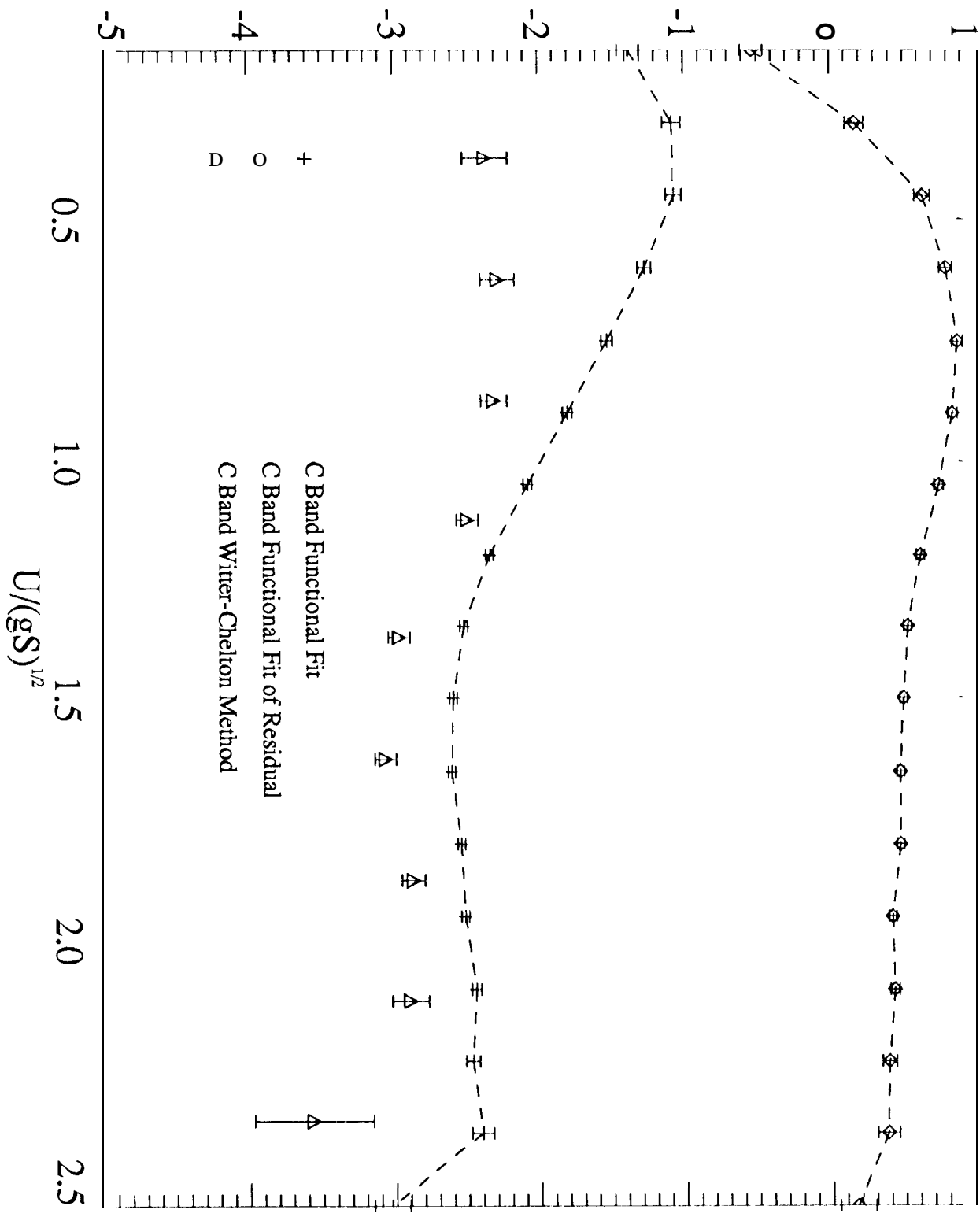


Figure 50